Photopolymerizable Liquid Encapsulants for Microelectronic Devices: Thermal and Mechanical Properties of Systems with Reduced In-Mold Cure Times

KIRAN K. BAIKERIKAR,[1] ALEC B. SCRANTON[2]

[1] Michigan State University, Department of Chemical Engineering, 2527 Engineering Building, East Lansing, Michigan 48824

[2] University of Iowa, Department of Chemical and Biochemical Engineering, 125 Chemistry Building, Iowa City, Iowa 52242

Received 10 May 2000; accepted 15 October 2000

ABSTRACT: Photopolymerizable liquid encapsulants (PLEs) for microelectronic devices may offer important advantages over traditional transfer molding compounds, including reduced in-mold cure times, lower thermal stresses, and reduced wire sweep. In this contribution, we discuss an encapsulation process based upon a low viscosity resin that cures rapidly upon exposure to UV light. These highly filled PLEs are comprised of an epoxy novolac-based vinyl ester resin (~25 wt %), fused silica filler (70–74 wt %), photoinitiator, silane coupling agent, and, in some cases, a thermal initiator. We have characterized the material properties (flexural strength and modulus, coefficient of thermal expansion, glass transition temperature, and thermal stress parameter) of PLEs cured with UV illumination times of 60, 90, and 120 s, as well as, the thermal conductivity and adhesive peel strength of PLEs photocured for 90 s. In addition, we investigated the effect of the fused silica loading and the initiation scheme on these properties. The results indicate that the PLEs are very promising for microelectronic encapsulation. These liquid encapsulants cure (to an ejectable hardness) in 1 min for an initiating light intensity of 200 mW/cm^2, and exhibit appropriate values for the thermal and mechanical properties listed above. © 2001 John Wiley & Sons, Inc. J Appl Polym Sci 81: 3449–3461, 2001

Key words: photopolymerization; liquid encapsulant; UV curing; microelectronic devices; plastic packaging

INTRODUCTION

Plastic encapsulated microelectronic devices consist of a silicon chip that is physically attached to a lead frame, electrically interconnected to input–output leads, and molded in a plastic that is in direct contact with the chip, lead frame, and interconnects.[1] The plastic is often referred to as the molding compound or encapsulant, and is used to protect the chip from adverse mechanical, thermal, chemical, and electrical environments. Encapsulation of microelectronic devices is typically accomplished using a transfer molding process in which the molding compound is cured by heat. In this process, the thermoset molding com-

Correspondence to: A. B. Scranton; (alec-scranton@uiowa.edu).

Journal of Applied Polymer Science, Vol. 81, 3449–3461 (2001)

pound (typically a solid epoxy preform) is dielectrically preheated and then placed into the pot of the molding tool. A transfer cylinder, or plunger, is used to push the molding compound into the runner system and gates of the mold. The molding compound then flows over the chips, wire bonds, and lead frames, encapsulating the entire assembly. After 2 to 3 min at approximately 175°C, the epoxy molding compound is cured to a sufficient degree of conversion (typically 60 to 90%) in the mold. Once the molding compound has reached an ejectable hardness, the encapsulated devices are removed from the mold and postcured for 4 to 8 h at 175°C to fully develop the material properties of the encapsulant.

In conventional transfer molding processes, the in-mold cure consumes the majority of the cycle time. For this reason, reducing the in-mold cure time of molding compounds is the most efficient way to reduce cycle times and increase productivity. For example, the in-mold cure time consumes approximately 70% of the overall cycle time, and an in-mold cure time reduction of even 15 s can translate to a productivity increase of about 10%.[2] With conventional systems, the cure time required before the parts can be ejected from the mold varies from 2 to 3 min. However, future developments will require in-mold cure times to be in the range of 60–90 s to achieve an overall cycle time of 2 min.[2]

Photopolymerizable liquid encapsulants (PLEs) are promising for reducing the in-mold cure time compared to the conventional thermal systems. These highly filled PLEs are comprised of an epoxy novolac-based vinyl ester resin (~25 wt %), fused silica filler (70–74 wt %), photoinitiator, thermal initiator, and silane coupling agent. As was shown in a previous article,[3] PLE samples containing a thermal initiator that were photocured for 120 s and then postcured for 6 h have the necessary material properties required by the microelectronics industry. These results demonstrate that an in-mold cure time of 2 min is achievable using PLEs. However, because future productivity requirements necessitate even faster in-mold cure times, the objective of this contribution is to determine if the UV illumination time (which corresponds to the in-mold cure time) for the PLEs can be reduced even further (while still retaining the 6 h postcure step at 170°C). Specifically, in this article we will examine the material properties (flexural strength and modulus, coefficient of thermal expansion, glass transition temperature, and thermal stress parameter) of PLEs cured with UV illumination times of 60, 90, and 120 s, as well as, the thermal conductivity and adhesive peel strength of PLEs photocured for 90 s. In addition, both UV initiation (using only a photoinitiator) and dual initiation (using both a photo and thermal initiator) results will be examined.

EXPERIMENTAL

Preparation of Photopolymerizable Liquid Encapsulant

The photopolymerizable liquid encapsulant is comprised of a base resin, photoinitiator, thermal initiator, fused silica filler, and silane coupling agent. The base resin used in these studies was DERAKANE 470-45 (Dow Chemical), an epoxy novolac-based vinyl ester resin that was chosen primarily for its low initial viscosity (0.0456 Pa · s or 45.6 cP at 30°C), as well as its appropriate thermal and mechanical properties upon cure. The photoinitiator used was bis(2,4,6-trimethylbenzoyl) phenylphosphine oxide (IRGACURE 819, Ciba). This photoinitiator, which we will henceforth denote as BAPO, has been shown to be especially appropriate for curing relatively thick polymers and composites due to its efficient photobleaching in the wavelength range of 360–450 nm.[4,5] The thermal initiator, benzoyl peroxide (Aldrich), was also used to determine the effects of a dual initiation scheme on the resulting material properties. The fillers used were all crushed (angular), untreated fused silica obtained from Minco, Inc. Fused silica was selected because it is the most commonly used filler in transfer molding compounds and it possesses the optimum combination of properties. Fused silica products with two different particle size distributions were used: (1) MIN-SIL 40 (median particle size = 22.11 μm), and (2) MIN-SIL 550 (median particle size = 6.03 μm). Typical compositions used a 50 : 50 wt % blend of MIN-SIL 40 to MIN-SIL 550 for a particular filler loading, as this was found to result in a formulation with a low initial viscosity and improved processability.[6] In addition, a silane coupling agent, 3-methacryloxypropyl-trimethoxysilane (Z-6030, Dow Corning), was used to provide a stable bond between the base resin and the fused silica filler, as well as, to improve the

processability of the liquid encapsulant formulation.

Photocurable formulations were prepared by adding 0.2 wt % (based on resin weight) of BAPO photoinitiator to DERAKANE 470-45 resin and stirring at room temperature on a magnetic stir plate until the photoinitiator completely dissolved. This amount of photoinitiator was selected because it was demonstrated in an earlier work to be the optimal concentration with regard to the final properties obtained.[4] The silane coupling agent was then added dropwise to the desired 1.0 wt % (based on filler weight) and the formulation was again mixed. Fused silica in the amount of 70.0, 72.0, or 74.0 wt % was added to the formulation and mixed by using a vortex mixer until the filler was completely dispersed and a homogeneous mixture was achieved. All resultant formulations were flowable liquids with viscosities of 5.9, 13.9, and 30.0 Pa · s (corresponding to 70.0, 72.0, and 74.0 wt % fused silica, respectively). After mixing, the formulation was degassed in a vacuum oven. Once these steps were completed, the photocurable formulation was ready to use for preparing samples required for the material property characterization studies.

To determine the effects of a dual initiation scheme, the thermal initiator, benzoyl peroxide, was also added to the liquid formulation. In this case, benzoyl peroxide in the amount of 1.2 wt % (based on resin weight) was added (after the photoinitiator had completely dissolved) and stirred until complete dissolution.

Flexural Strength and Modulus

Specimens for flexural testing were prepared by photopolymerizing the liquid encapsulant formulation in rectangular-shaped silicone molds with unfiltered UV light of 200 mW/cm^2 UVA intensity from a 3000 W arcless mercury vapor lamp (Fusion UV Systems, model F450T). Light intensities were measured using a UVICURE Plus high energy UV integrating radiometer (over the 320–390 nm range). Specimens were 76.2 mm length $\times$ 12.7 mm width $\times$ 3.2 mm depth, and were photocured for various times (60, 90, and 120 s). To fully develop the material properties, specimens were postcured at 170°C in a laboratory oven for 6 h after UV curing.

The flexural strength and modulus of the photocured samples were determined using a United SFM-20 instrument in accordance with the ASTM D 790 method. The flexural properties were measured using the three point flexural test with a span length of 50.8 mm (2 inches), a 454-kg (1000 lb.) load cell, and a downdrive rate of 1.9 mm/min (0.07 in/min). Flexural strength and modulus values were calculated using DATUM 97 software (United Testing Systems).

Coefficient of Thermal Expansion and Glass Transition Temperature

Specimens for coefficient of thermal expansion (CTE) testing were cut from the samples used for flexural testing so that the thermal stress parameter of the photocured encapsulants could be estimated. Dimensions of the cut-away samples were approximately 11 mm length $\times$ 8 mm width $\times$ 3.2 mm thickness. All samples were cut using a diamond wafering saw. The CTE below the glass transition (α_1) and CTE above glass transition (α_2) were both measured using a DuPont 943 thermomechanical analyzer (TMA) interfaced with a DuPont model 9900 thermal analyzer controller. The photopolymerized samples were heated from room temperature (23°C) to 234°C at a constant rate of 3°C/min. The change in the sample thickness during heating was recorded in the personal computer, and α_1 was obtained from the inclined line connecting two points on the TMA curve, 50 and 70°C. To determine α_2, the inclined line connecting 200 and 230°C was used. The glass transition temperature was taken to be the temperature at the intersection of these two lines.

Thermal Conductivity

Specimens for thermal conductivity testing were prepared by photopolymerizing the liquid encapsulant in rectangular silicone molds with unfiltered UV light (200 mW/cm^2 UVA intensity) for 90 s from the 3000-W arcless mercury vapor lamp. Following UV illumination, the specimens were postcured in a laboratory oven for 6 h at 170°C. The final dimensions of the cured specimens were 76.2 mm length, 25.4 mm width, and 3.2 mm depth. The cured specimens were then machined into disks with a diameter of 12.7 mm and a thickness of 1.0 mm for thermal conductivity testing.

All measurements to determine the thermal conductivity by the laser flash method were performed by Holometrix, Inc. (Bedford, MA) using

the Holometrix Thermaflash 2200 Laser Flash system and in accordance with the ASTM E1461-92 method. The laser flash method for determining thermal conductivity has been applied to a wide range of materials, including composites, plastics, ceramics, metals, glasses, crystals, and foams. One advantage of this technique is that it requires only a small amount of material. In this technique, the measurement of the thermal diffusivity of a material is carried out by rapidly heating one side of the flat disk sample and measuring the temperature as a function of time (the temperature rise curve) on the opposite side. Based upon this temperature profile, the through-plane diffusivity is measured, and the thermal conductivity is calculated using the known values of the specific heat and bulk density.[7]

In these studies, the sample disk made from the PLE was aligned between a neodymium glass laser (1.06 μm wavelength) and an indium antimonide (InSb) IR detector in a tantalum tube furnace. To prevent penetration of the laser beam into the sample, the PLE samples were coated with a 0.1-μm gold film. In addition, because the PLE samples do not have a high value of emissivity or absorptivity, the samples were also coated with a 5-μm graphite film before testing. The graphite film increases the energy absorbed on the laser side and increases the temperature signal on the rear face of the sample. A Type C thermocouple in contact with the PLE sample was used to control the temperature of the sample and its surroundings between 20 and 2000°C. Once the sample was stabilized at 25°C, the laser was fired several times over a span of a few minutes, and the necessary data was recorded for each laser shot. The laser energy is absorbed by the front surface of the sample, causing a heat pulse to travel through the thickness of the sample. The resulting sample temperature rise is fairly small (ranging from about 0.5 to 2°C), and is kept in the optimal range by adjustable filters between the laser and the furnace. A lens focuses the back surface image of the sample onto the IR detector and the temperature rise signal vs. time is amplified and recorded with a high speed A/D converter. The thermal diffusivity is determined from a numerical analysis of the IR detector output. In addition, the specific heat can be measured with the laser flash method by comparing the temperature rise of a reference sample of known specific heat tested under the same conditions.[7] The instrument is fully automated to control all systems and record, analyze, and report the thermal diffusivity, specific heat, and the calculated thermal conductivity.

Adhesion

Solvent Degreasing Pretreatment of Alloy 194

The degree of adhesion between the photopolymerizable liquid encapsulants (PLEs) and the leadframe metal was measured by the 180° peel test, as this method has been shown to be an accurate measure of adhesion between the encapsulants and the leadframe.[8] Alloy 194 was selected as the lead frame metal for the 180° peel test because of its widespread use in microelectronic packages. It is a copper-based lead frame metal, comprised of 97.5% copper, 2.35% iron, 0.12% zinc, and 0.03% phosphorus.[2] Thin foil sheets of Alloy 194 (C194, Olin Brass) with thickness 0.0127 mm (0.0005 in.) were cut into rectangular strips of dimensions 215.9 mm (8.5 in.) length and 12.7 mm (0.5 in.) width. The thin foil was necessary for the peel test to permit a turn back at an approximate 180° angle in the expected loading range of the test without failure. Prior to applying the PLE to the leadframe metal, the copper alloy was pretreated to provide a surface to which the resin can adhere. Typically, metals available for industrial applications are covered with a contaminant layer that has properties that differ from the bulk metal and, consequently, this alters the degree of adhesion between the metal and polymer. The contaminant layer may consist of processing lubricants and oils, water, or other contaminants from the atmosphere that can adsorb on the high energy metal surfaces.[9] A solvent degreasing pretreatment is typically the minimum pretreatment used to remove this contaminant layer.

The Alloy 194 strips were cleaned and degreased by first dipping them in 0.1 *M* HCl for 30 s to remove the weak copper oxide, then rinsing with a series of solvents in the following order: distilled water; methanol; distilled water; acetone. The strips were then dried gently with compressed air. Environmental scanning electron microscopy (ESEM) was conducted to determine the surface characteristics of the foils. The microscope was a Philips Electroscan 2020 environmental scanning electron microscope (ESEM)

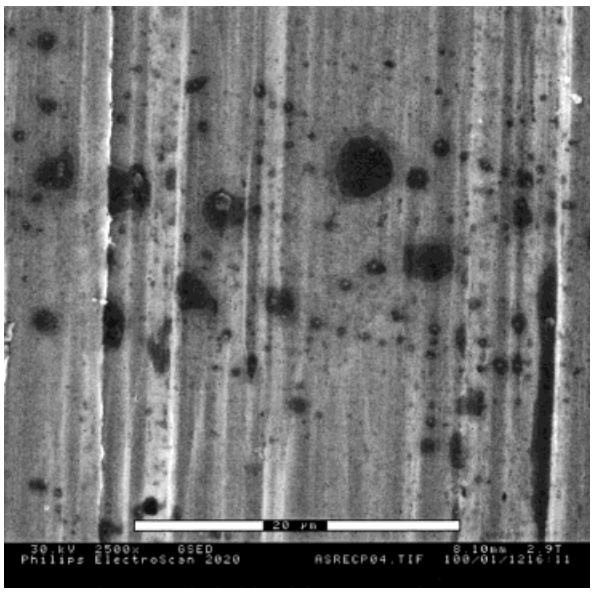

Figure 1 Scanning electron micrograph of Alloy 194 before cleaning.

equipped with a Lab6 filament. The accelerating voltage was 20 kV and the operating pressure ranged between 2–3 Torr. Scanning electron micrographs of leadframe strips before and after pretreatment are shown in Figures 1 and 2, respectively. Figure 1 shows the dirt and oil (dark-colored circles) on the "as-received" Alloy 194 strips, confirming that a pretreatment step is necessary to clean the surface and adequately prepare it for adhesion. Figure 2 shows a much cleaner surface after the Alloy 194 strips were pretreated, demonstrating that the pretreatment was successful in removing the surface contaminants. Following pretreatment, the Alloy 194 strips were primed with silane coupling agents, as this has been shown by other authors to be effective in improving the peel strength.[10]

Treatment of Alloy 194 Strips with Silane Coupling Agents

Two different silane coupling agents were used for priming the copper surfaces, 3-methacryloxypropyltrimethoxysilane (Z-6030, Dow Corning) and a silane composed of an amino-alkyltrimethoxysilane and a polyol diluted with methanol (Z-6026, Dow Corning). These coupling agents, Z-6030 and Z-6026, will henceforth be denoted as MPMS and AAMS, respectively. Coupling agent solutions using MPMS were made to a concentration of 5.0 wt % in methanol. Alloy 194 strips were dipped in the solution for 1 min, removed, blown gently with air, and cured at 115°C for 30 min.

Coupling agent solutions using AAMS were made to a concentration of 0.5 wt % in water. The pH was then adjusted to 4.5 with acetic acid. Alloy 194 strips were dipped in the solution for 1 min, removed, gently blown with air, and cured at 115°C for 30 min.

Specimen Preparation for Peel Test

Following pretreatment, the Alloy 194 strips were inserted into rectangular cavities of a Teflon mold, with cavity dimensions of 101.6 mm (4 in.) length, 12.7 mm (0.5 in.) width, and 3.5 mm (0.1378 in.) depth. The PLE was then injected, using a syringe, into the mold cavities and allowed to completely wet the metal strips. The specimens were photopolymerized for 90 s with unfiltered UV light of 200 mW/cm^2 UVA intensity from the 3000 W arcless mercury vapor lamp to create a bond length of 101.6 mm (4 in.) between the metal and photocured encapsulant. After photocuring, the samples were allowed to cool to room temperature for 24 h prior to the peel test. The peel test was performed by peeling off the thin leadframe foil at a 180° angle from the photocured encapsulant with a United SFM-20 instrument at a rate of 127 mm/min (5 in./min) and a 9.07 kg (20

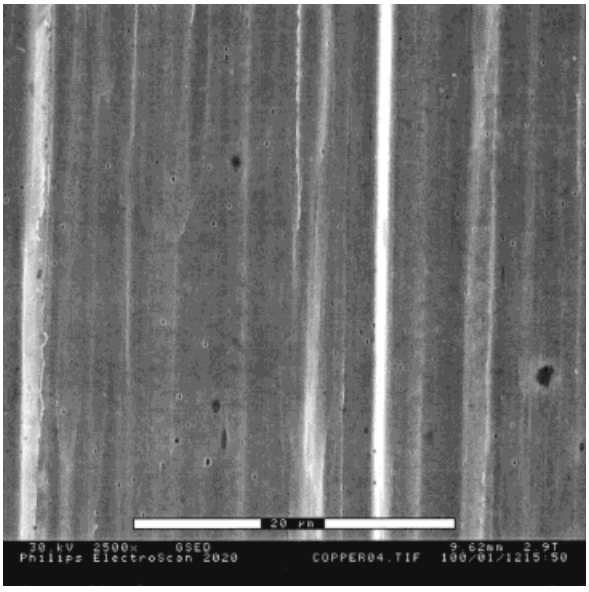

Figure 2 Scanning electron micrograph of Alloy 194 after cleaning.

Table I Effect of Reduced UV Illumination Times on Flexural Modulus for Both UV-Initiated and Dual Initiated Samples Containing 70.0, 72.0, and 74.0 wt % Fused Silica

UV Illumination Time (s)	Wt % Fused Silica	Flexural Modulus (kg_f/mm^2) without Thermal Initiator	Flexural Modulus (kg_f/mm^2) with Thermal Initiator
60	70.0	988 ± 50	1060 ± 132
60	72.0	1164 ± 72	1118 ± 82
60	74.0	1209 ± 99	1247 ± 66
90	70.0	945 ± 44	967 ± 60
90	72.0	1024 ± 111	1120 ± 158
90	74.0	1254 ± 137	1234 ± 109
120	70.0	1059 ± 111	973 ± 89
120	72.0	1160 ± 62	1139 ± 124
120	74.0	1240 ± 97	1207 ± 117

Samples were photocured with UV light of 200 mW/cm^2 UVA intensity and then postcured for 6 h at 170°C.

lb.) load cell. Peel strength was calculated using DATUM 97 software (United Testing Systems).

RESULTS AND DISCUSSION

Flexural Strength and Modulus

Encapsulants must have excellent mechanical properties in order to withstand mechanical shock, vibration, and handling during assembly. One of the more important mechanical properties is the flexural modulus, which characterizes the stiffness of a material under an applied load (it is the slope of a plot of stress versus strain in the elastic portion of the curve).[11] By reducing the flexural modulus, the thermal stress (also known as the stress parameter) is also reduced, and recent research indicates that this leads to improved device reliability. In particular, this stress causes interfacial cracking and breakage of wire bond leading, as well as passivation layer cracking and aluminum pattern deformation.[12,13] To reduce the thermal shrinkage stresses, a flexural modulus near or below 1000 kg_f/mm^2 (9806.6 MPa) is recommended.[2]

Effect of Reduced UV Illumination Times on Flexural Modulus and Strength

Table I shows the effect of reduced UV illumination times on flexural modulus for both UV-initiated and dual initiated samples containing 70.0, 72.0, and 74.0 wt % fused silica. Each entry in Table I represents the average of five samples, and the indicated range corresponds to one standard deviation above and below the mean. All samples contained 70.0 to 74.0 wt % fused silica, 1.0 wt % silane coupling agent (based on filler weight), 0.2 wt % BAPO (based on resin weight), 1.2 wt % benzoyl peroxide (based on resin weight), and the balance epoxy novolac-based vinyl ester resin. Samples were photocured with UV light of 200 mW/cm^2 UVA intensity and then postcured for 6 h at 170°C in a laboratory oven. From Table I, it can be seen that a reduction in UV illumination time from 2 min to 1 min followed by postcure has no deleterious effect on the flexural modulus of the PLEs. All of the PLEs (including those cured for only 60 s) had sufficient green strength to maintain their shape and integrity when ejected from the mold. In addition, after postcure, all samples exhibited flexural modulus values near the desired value of 1000 kg_f/mm^2 (9806.6 MPa). For example, flexural modulus values for samples filled with 70.0 wt % fused silica ranged from 940 to 1060 kg_f/mm^2 (9218 to 10,395 MPa), those with 72.0 wt % fused silica had modulus values between 1020 and 1160 kg_f/mm^2 (10,003 to 11,376 MPa), and samples filled with 74.0 wt % fused silica had values between 1200 and 1260 kg_f/mm^2 (11,768 to 12,356 MPa). In addition, the inclusion of the thermal initiator has no effect on the flexural modulus.

Table II illustrates the effect of reduced UV illumination times on flexural strength for both UV-initiated and dual initiated samples containing 70.0, 72.0, and 74.0 wt % fused silica. From Table II, two findings are evident. First, the inclusion of the thermal initiator increases the flexural strength of the PLEs, typically by 1 to 2 kg_f/mm^2 (9.81 to 19.61

Table II Effect of Reduced UV Illumination Times on Flexural Strength for Both UV-Initiated and Dual Initiated Samples Containing 70.0, 72.0, and 74.0 wt % Fused Silica

UV Illumination Time (s)	Wt % Fused Silica	Flexural Strength (kg_f/mm^2) without Thermal Initiator	Flexural Strength (kg_f/mm^2) with Thermal Initiator
60	70.0	7.18 ± 1.61	8.72 ± 0.97
60	72.0	8.37 ± 1.38	9.41 ± 0.95
60	74.0	8.87 ± 1.30	9.80 ± 1.55
90	70.0	7.88 ± 0.71	9.07 ± 0.73
90	72.0	8.41 ± 0.83	8.75 ± 1.00
90	74.0	8.29 ± 1.13	11.11 ± 1.09
120	70.0	6.71 ± 0.69	8.83 ± 1.68
120	72.0	7.59 ± 0.24	9.28 ± 0.95
120	74.0	8.12 ± 0.69	9.92 ± 1.44

Samples were photocured with UV light of 200 mW/cm^2 UVA intensity and then postcured for 6 h at 170°C.

MPa). The flexural strength values for samples with the thermal initiator, again, meet the requirements for molding compounds (flexural strength values of at least 9 kg_f/mm^2 or 88 MPa). Second, the flexural strengths for UV illumination times of 60 and 90 s are essentially equivalent to the values of 120 s. This is further evidence that the in-mold cure time of the PLEs can be successfully reduced to 60 s.

Effect of Reduced UV Illumination Times on the Coefficient of Thermal Expansion and Glass Transition Temperature

The linear coefficient of thermal expansion (CTE) is defined as the ratio of the change in the length of the sample to the change in temperature per unit initial length.[14] This parameter is very important in semiconductor encapsulation because a significant CTE mismatch between the encapsulant, lead frame, and the silicon chip can lead to the build up of internal stresses in the semiconductor device, and could lead to cracking of the chip or encapsulant. Current encapsulants exhibit α_1 values (CTE below glass transition) in the range of 15–30 $\mu m/m°C$, while copper lead frames possess a value of 16–17 $\mu m/m°C$ and silicon exhibits a value of 3–4 $\mu m/m°C$.[15] The service temperature for microelectronic encapsulants is typically between 75 and 85°C, which is well below the glass transition temperature of the encapsulant.[2] For this reason, the value of the CTE above the glass transition temperature, α_2, is not as important as the CTE below the glass transition temperature, α_1. The glass transition temperature of microelectronic encapsulants is typically between 140 to 180°C.

Table III shows the effect of reduced UV illumination times on the coefficient of thermal expansion below glass transition for samples that were photocured with UV light of 200 mW/cm^2 UVA intensity and then postcured for 6 h at 170°C. Again, each entry in Table III represents the average of five samples and the indicated range corresponds to one standard deviation above and below the mean. All samples contained 70.0 to 74.0 wt % fused silica, 1.0 wt % silane coupling agent (based on filler weight), 0.2 wt % BAPO (based on resin weight), 1.2 wt % benzoyl peroxide (based on resin weight), and the balance

Table III Effect of Reduced UV Illumination Times on Coefficient of Thermal Expansion Below Glass Transition for Both UV-Initiated and Dual Initiated Samples Containing 70.0, 72.0, and 74.0 wt % Fused Silica

UV Illumination Time (s)	Wt % Fused Silica	α_1 ($\mu m/m°C$) without Thermal Initiator	α_1 ($\mu m/m°C$) with Thermal Initiator
60	70.0	22.10 ± 1.57	20.84 ± 1.35
60	72.0	19.80 ± 0.87	20.20 ± 1.43
60	74.0	20.02 ± 1.27	19.36 ± 1.23
90	70.0	22.04 ± 0.71	22.30 ± 1.26
90	72.0	19.40 ± 1.21	20.20 ± 0.51
90	74.0	18.58 ± 0.45	19.44 ± 1.20
120	70.0	22.26 ± 0.63	22.70 ± 1.10
120	72.0	22.62 ± 0.64	20.92 ± 0.54
120	74.0	20.50 ± 0.57	20.12 ± 1.41

Samples were photocured with UV light of 200 mW/cm^2 UVA intensity and then postcured for 6 hours at 170°C.

Table IV Effect of Reduced UV Illumination Times on Glass Transition Temperature for Both UV-Initiated and Dual Initiated Samples Containing 70.0, 72.0, and 74.0 wt % Fused Silica

UV Illumination Time (s)	Wt % Fused Silica	T_g (°C) without Thermal Initiator	T_g (°C) with Thermal Initiator
60	70.0	156 ± 2	155 ± 2
60	72.0	153 ± 1	154 ± 2
60	74.0	153 ± 2	153 ± 1
90	70.0	152 ± 1	149 ± 2
90	72.0	152 ± 2	150 ± 2
90	74.0	150 ± 1	150 ± 2
120	70.0	148 ± 2	150 ± 2
120	72.0	150 ± 4	151 ± 1
120	74.0	152 ± 3	150 ± 1

Samples were photocured with UV light of 200 mW/cm^2 UVA intensity and then postcured for 6 h at 170°C.

epoxy novolac-based vinyl ester resin. Samples were photocured with UV light of 200 mW/cm^2 UVA intensity and then postcured for 6 h at 170°C in a laboratory oven. From Table III, again, there is no significant difference in α_1 between specimens photopolymerized for 60 s (and then postcured for 6 h) and specimens photopolymerized for 90 and 120 s (and then postcured for 6 h). This is to be expected, because the reduction in the coefficient of thermal expansion occurs primarily in the postcure step. In addition, the addition of the thermal initiator has little effect on α_1.

Table IV shows the effect of reduced UV illumination times on the glass transition temperature (T_g) for samples that were photocured with UV light of 200 mW/cm^2 UVA intensity and then postcured for 6 h at 170°C. The T_g values range between 152 and 155°C for samples that were photocured for 60 s and postcured for 6 h, while the observed T_g values fell between 148 and 152°C for samples that were photocured for 90 and 120 s (and then postcured for 6 h). Therefore, the glass transition temperature for all of the PLE samples is near 150°C, and is within the required range for microelectronic encapsulants.

Effect of Reduced UV Illumination Times on Thermal Stress Parameter

As was mentioned previously, lowering the stress parameter leads to improved device reliability. The thermal stress parameter, σ^*, is typically calculated using the following equation:[2]

$$\sigma^* = (\alpha_{pg} - \alpha_i)E_{pg}(T_g - T_1) \quad (1)$$

Here, α_{pg} represents the coefficient of thermal expansion below glass transition of the encapsulation material, α_i is the coefficient of thermal expansion of the silicon device or metal leadframe, E_{pg} is the modulus of elasticity (tensile or flexural) of the encapsulant, and T_g is the glass transition temperature of the encapsulant (°C). To evaluate the thermal stress parameter for the photopolymerized encapsulants of this study, the experimental values for α_{pg}, E_{pg} (flexural), and T_g were substituted into this equation along with literature values for α_i and T_1. Specifically, we used the CTE of a copper metal lead frame (16.3 μm/m °C) for α_i and −65°C for T_1, because this is the usual starting temperature for temperature cycling tests as specified by Mil. Std. 38510 Group D.[2]

Table V shows the effect of reduced UV illumination times on the calculated thermal stress parameter (σ^*) for samples that were photocured with UV light of 200 mW/cm^2 UVA intensity and then postcured for 6 h at 170°C. Thermal stress parameter values are the average of five samples, and the indicated range corresponds to one standard deviation. The relatively high degree of un-

Table V Effect of Reduced UV Illumination Times on Thermal Stress Parameter (σ^*) for Both UV-Initiated and Dual Initiated Samples Containing 70.0, 72.0, and 74.0 wt % Fused Silica

UV Illumination Time (s)	Wt % Fused Silica	σ^* (kg_f/mm^2) without Thermal Initiator	σ^* (kg_f/mm^2) with Thermal Initiator
60	70.0	1.27 ± 0.37	1.06 ± 0.38
60	72.0	0.88 ± 0.21	0.95 ± 0.36
60	74.0	0.99 ± 0.39	0.84 ± 0.36
90	70.0	1.18 ± 0.18	1.24 ± 0.24
90	72.0	0.68 ± 0.23	0.95 ± 0.23
90	74.0	0.62 ± 0.17	0.84 ± 0.34
120	70.0	1.34 ± 0.20	1.35 ± 0.32
120	72.0	1.58 ± 0.20	1.14 ± 0.23
120	74.0	1.13 ± 0.19	1.05 ± 0.38

Samples were photocured with UV light of 200 mW/cm^2 UVA intensity and then postcured for 6 h at 170°C.

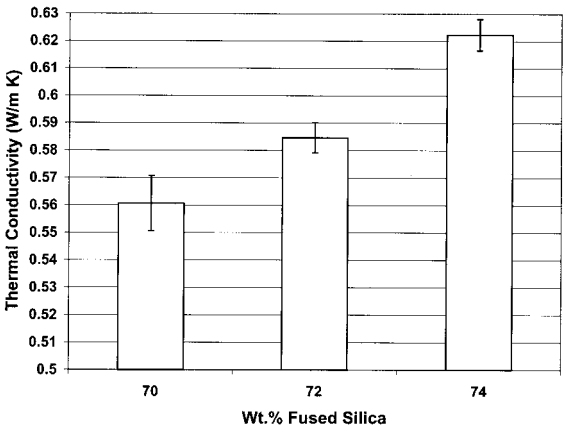

Figure 3 Thermal conductivity of PLEs at 25°C as a function of fused silica loading.

certainty in the values of σ^* shown in Table V arises from the combined uncertainty of the three material properties used in the calculation. As the value of σ^* increases, the likelihood of thermally induced stresses also increases. Therefore, low values of σ^* are desired. Conventional microelectronic encapsulants typically exhibit thermal stress parameters anywhere between 0.50 and 1.50 kg_f/mm^2 (4.90 and 14.71 MPa). The data in Table V illustrate that the PLEs in this study generally exhibit σ^* values ranging from 0.6 to 1.3 kg_f/mm^2 (5.88 to 12.75 MPa), and are therefore within the range exhibited by current encapsulants.

Thermal Conductivity

Because the device generates a significant amount of heat during use, the thermal conductivity of an encapsulating compound plays an important role in the thermal management of the device. Indeed, the thermal conductivity determines the amount of heat that can be removed from the device, and thus affects operating temperatures of electronic components.

Experimental data showing the thermal conductivity of the PLEs as a function of fused silica loading are shown in Figure 3. All samples contained 70.0 to 74.0 wt % fused silica, 1.0 wt % silane coupling agent (based on filler weight), 0.2 wt % BAPO (based on resin weight), 1.2 wt % benzoyl peroxide (based on resin weight), and the balance epoxy novolac-based vinyl ester resin. Samples were photocured for 90 s with UV light of 200 mW/cm^2 UVA intensity and then postcured for 6 h at 170°C. Each bar in the bar chart represents the average of three samples, and the error bars indicate one standard deviation above and below the mean. As expected, the thermal conductivity of the PLEs increases as the fused silica content is increased, and the values range between 0.56 and 0.62 W/m · K. Clearly, the thermal conductivity of a molding compound is largely dependent on the filler used and, therefore, the thermal conductivity values of the PLEs filled with fused silica (k = 1.5 W/m · K) will not be as high as molding compounds loaded with higher thermal conductivity fillers, such as silicon carbide (k = 85 W/m · K), aluminum nitride (k = 150–220 W/m · K), and boron nitride (k = 250–300 W/m · K). However, the thermal conductivity values of the PLEs are all within the 0.5 to 0.7 W/m · K range of epoxy molding compounds filled with fused silica. As a result, the PLEs are more suitable for applications with low stress requirements, rather than devices with high heat outputs.

To predict the thermal conductivity of encapsulants at higher filler loadings, theoretical and empirical models are often used. Although other additives are typically present in encapsulants, such as initiators and coupling agents, the concentration added is rather small when compared to that of the fillers. Thus, from a thermal transport point of view, the encapsulant behaves like a two-phase composite.[16] Several second-order models have been developed to predict the thermal conductivity of a two-phase composite (Agari and Uno,[17] Hatta and Taya,[18] Hashin and Shtrikman,[19] and Nielsen[20]); the model developed by Agari and Uno describes the thermal conductivity of encapsulants quite well.[21,22] Indeed, the model is especially suited for composites with high filler loadings (30 to 60 vol %) and irregularly shaped filler particles, such as fused silica. The model is described by eq. (2):

$$\log k_c = \phi C_2 \log(k_f) + (1 - \phi)\log(C_1 k_m) \qquad (2)$$

and can be rearranged to give eq. (3):

$$k_c = k_f^{\phi C_2}[(C_1 k_m)^{(1-\phi)}] \qquad (3)$$

where k_c, k_f, and k_m are the thermal conductivities of the composite, filler, and resin matrix, respectively, and ϕ is the volume fraction of the filler. In addition, C_1 is a constant used to measure the effect of filler particles on the secondary

Table VI Calculated Volume Fractions Corresponding to 70.0, 72.0, and 74.0 wt % Fused Silica Loadings

Weight Fraction Fused Silica W	Volume Fraction Fused Silica ϕ
0.70	0.526
0.72	0.551
0.74	0.576

structure of the resin matrix and C_2 is a constant used to measure the ease with which the filler particles begin to form conductive chains.[17] For the purpose of modeling the thermal conductivity of the PLEs, known values for the thermal conductivities of fused silica (k_f = 1.5 W/m · K) and the epoxy novolac-based vinyl ester resin (k_m = 0.182 W/m · K) were used. The fused silica volume fractions, ϕ, were calculated using eq. (4):

$$\phi = \frac{W}{W + (1 - W)\dfrac{\rho_f}{\rho_m}} \tag{4}$$

where W is the weight fraction of fused silica, ρ_f is the density of the filler (ρ_f = 2.20 g/cm^3 for fused silica), and ρ_m is the density of the resin matrix (ρ_m = 1.048 g/cm^3 for epoxy novolac-based vinyl ester resin). Table VI shows the calculated volume fractions corresponding to the 70.0, 72.0, and 74.0 wt % fused silica loadings. Once the volume fractions were determined, the experimental thermal conductivity data was fit to eq. (3) by nonlinear regression using C_1 and C_2 as the fitting parameters. The nonlinear regression analysis was performed using the commercial software package Origin 5.0 (Microcal Software, Inc.).

Figure 4 compares the experimental thermal conductivity results to the predicted values obtained using the model of Agari and Uno. The curve drawn in Figure 4 corresponds to values obtained by fitting the experimental data to eq. (3), from 0 to 80.0 wt % fused silica (0 to 65.6 vol %). The best fit values for C_1 and C_2 were 0.997 and 1.064, respectively. These values are quite reasonable, because C_1 values reported by Agari and Uno for various composite systems are approximately 1, and C_2 values range from 1 to 1.5.[23] A value of C_1 close to 1 implies that the secondary structure of the epoxy novolac-based vinyl ester resin is essentially unaffected by the fused silica particles.[23] Figure 4 demonstrates that the experimental thermal conductivity data is well correlated by the model of Agari and Uno. The model can be used to effectively predict the thermal conductivity of the PLEs at both lower and higher filler loadings. For example, the model predicts that the thermal conductivity of the PLEs will be 0.50 W/m · K at 66.0 wt % fused silica and 0.74 W/m · K at 80.0 wt % fused silica.

Adhesion

Peel Strength of Surfaces Treated with Silane Coupling Agents

Experimental results showing the 180° peel strength between the photopolymerizable liquid encapsulants and the Alloy 194 strips treated with the silane coupling agents are shown in Figure 5. Each bar in the bar chart represents the average of five samples, and the error bars indicate one standard deviation above and below the mean. As shown in Figure 5, the peel strength of strips that were not treated with silane coupling agents ranged from 18 to 40 g/cm. In addition, the peel strength of strips that were treated with MPMS ranged from 28 to 40 g/cm, demonstrating that the use of MPMS has a minimal effect in improving the peel strength. The only noticeable improvement shown by MPMS occurs when the liquid encapsulant is filled with 74.0 wt % fused silica. However, Figure 5 clearly shows that the use of AAMS significantly improves the peel

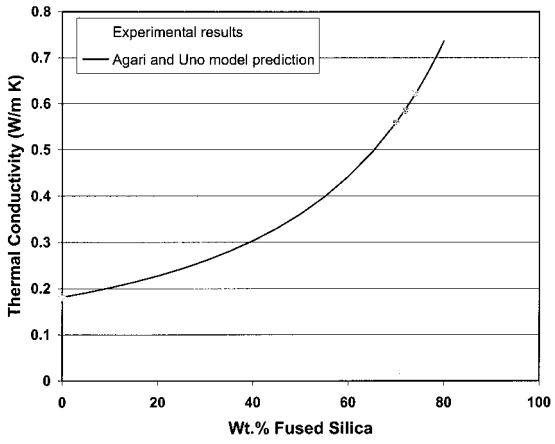

Figure 4 Comparison of experimental thermal conductivity results to the predicted values obtained using the model of Agari and Uno from 0 to 80.0 wt % fused silica (0 to 65 vol %).

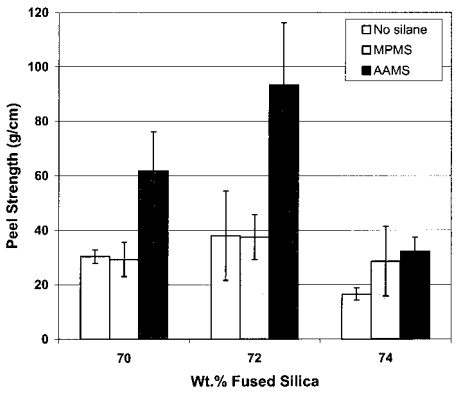

Figure 5 Peel strength between photopolymerizable liquid encapsultants and Alloy 194 strips treated with silane coupling agents.

strength, because the peel strength values for strips treated with AAMS were between 35 and 95 g/cm. At each level of filler loading, the peel strength is more than doubled for Alloy 194 strips that were treated with AAMS, compared to strips that were not treated with any silane coupling agent.

In addition, Figure 5 shows that irrespective of whether the Alloy 194 strips are treated with a silane coupling agent, the peel strength reaches a maximum when the photopolymerizable liquid encapsulant is filled with 72.0 wt % fused silica. This is somewhat unexpected, as other authors, most notably Kim, have shown that peel strength shows an inverse relationship with viscosity, i.e., the lower the viscosity the higher the peel strength.[8] The viscosity of the liquid encapsulant filled with 70.0 wt % fused silica is 5.92 Pa · s (5920 cP), while that of the 72.0 wt % encapsulant is 13.9 Pa · s (13,900 cP), and 74.0 wt % is over 30 Pa · s (over 30,000 cP).[6] Therefore, based solely upon this consideration, one would expect that the encapsulant filled with 70.0 wt % fused silica to exhibit the highest peel strength, followed by 72.0 wt %, and then 74.0 wt %. The discrepancy between the data shown in Figure 5 and the trend observed by Kim may be attributed to the manner in which the viscosity was varied. Kim altered the viscosity level by varying the catalyst levels and processing times, whereas we have varied the viscosity levels by solely varying the filler loading. As a result, there are two competing effects on the peel strength of the PLEs: viscosity and internal stress. It appears that the PLE filled with 72.0 wt % fused silica strikes the appropriate balance: it has a low enough viscosity to provide adequate wetting of the Alloy 194 strips, and enough fused silica to sufficiently reduce the internal stresses (which lower peel strength).

Commercial epoxy molding compounds generally exhibit 180 degree peel strengths of 40 to 200 g/cm when adhered to copper leadframe materials.[8] Figure 5 illustrates that the PLEs filled with 70.0 and 72.0 wt % fused silica and that are molded onto Alloy 194 strips treated with AAMS exhibit peel strength values in this range. Therefore, these studies indicate that these materials exhibit appropriate peel strength values for use as microelectronic encapsulants. In addition, it is noteworthy that the 180 degree peel strengths reported by Kim on the commercial encapsulants were performed using relatively thin samples (1.25 mm thick), whereas, the PLE specimens in this study were 3.0 mm thick (microelectronic encapsulants are generally 1–3 mm thick and we chose the high end of the range because it places the most stringent requirements upon cure and adhesion). Other investigators have shown that an increase in the encapsulant thickness can lead to increased internal stresses and decreased peel strengths.[24] Therefore, if the peel strengths of the PLEs and the commercial molding compounds were compared based upon identical specimen thicknesses, the PLEs should compare even more favorably than the values shown in Figure 5.

Mechanism of Bond Failure between PLE and Surfaces Treated with Silanes

Adhesive joints may fail in two ways: (1) adhesive failure, which is interfacial bond failure between the adhesive and the adherend (in this case the separation occurs at the adhesive-adherend interface), and (2) cohesive failure, in which a layer of adhesive remains on both surfaces (in this case separation occurs in the adhesive).[25] Cohesive failure is the desirable mode of failure because it indicates that the adhesive bond was strong enough to prevent failure at the interface.

In this study, the mode of the failure of the adhesive joint was investigated using environmental scanning electron microscopy (ESEM). Specifically, the Alloy 194 surface of the failed peel test specimen was examined. The ESEM micrographs reveal that all of the surfaces treated with either silane coupling agent as well as the control surfaces (strips that were cleaned and degreased, but were not treated with silanes) showed cohesive failure. For these systems, the

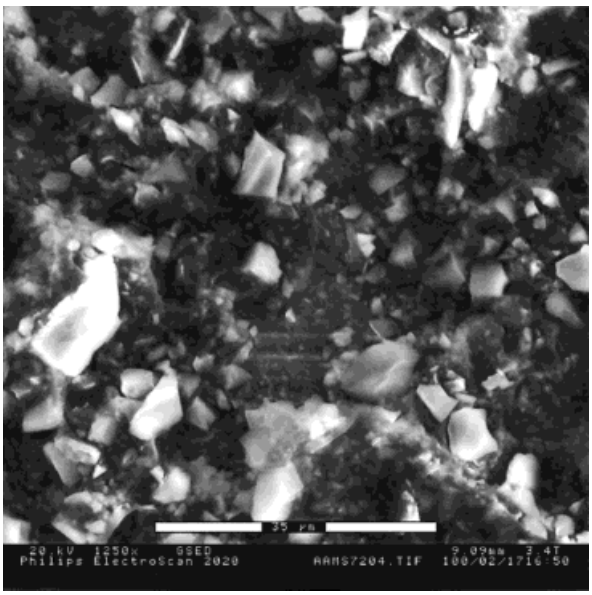

Figure 6 Scanning electron micrograph of the peel test specimen showing cohesive failure between PLE filled with 72 wt % fused silica and Alloy 194 strip treated with AAMS. The particles are remnants of the PLE adhered to the Alloy 194 surface after the 190 degree peel test.

micrographs indicate that a layer of the cured PLE remained on the Alloy 194 surface after the peel test, as shown by the representative micrograph in Figure 6.

CONCLUSIONS

Current trends in microelectronic encapsulation will require in-mold cure times for molding materials to be reduced from 120 s to 60–90 s. With current thermally cured systems this reduced cure time is difficult to achieve. In this article, we have shown that photopolymerizable liquid encapsulants (PLEs) comprised of an epoxy novolac-based vinyl ester resin (~25 wt %), fused silica filler (70–74 wt %), photoinitiator, silane coupling agent, and a thermal initiator can meet this requirement. Photopolymerizable liquid encapsulants that were photocured for 60 and 90 s had appropriate ejectable hardness, and upon post-cure, exhibited material properties (flexural strength and modulus, coefficient of thermal expansion, glass transition temperature, thermal stress parameter, thermal conductivity, and adhesive peel strength) that were equivalent or better than those of conventional encapsulants. It was also shown that the addition of a thermal initiator does not negatively affect any of the material properties, and leads to improved flexural strength.

We are grateful for the financial and instrumental support from the Composite Materials and Structures Center (CMSC) at Michigan State University and, in particular, appreciate the help of Dr. Richard Schalek for the ESEM pictures. Special thanks to Robert Campbell and Paul Ricci of Holometrix, Inc. for performing the thermal conductivity testing. Additional thanks go to Steve Beversluis of MINCO, Inc. for providing the fused silica, as well as, Scott Lindseth of Nitto Denko America, Inc. and Christine Naito of Dexter Electronic Materials for their help in answering specific questions about transfer molding compounds.

NOMENCLATURE

C_1 = constant used to measure the effect of the filler on the secondary structure of resin
C_2 = constant used to measure the ease with which filler particles begin to form conductive chains
E_{pg} = modulus of elasticity (flexural) of the encapsulant
k = thermal conductivity
k_c = thermal conductivity of composite
k_f = thermal conductivity of filler
k_m = thermal conductivity of resin matrix
T_g = glass transition temperature of encapsulant
W = weight fraction of filler
α_i = coefficient of thermal expansion of metal lead frame
α_{pg} = coefficient of thermal expansion below glass transition of encapsulation material
ϕ = volume fraction filler
ρ = density
ρ_f = density of filler
ρ_m = density of resin matrix

REFERENCES

1. Shinohara, M.; Electronic Materials Handbook; Minges, M. L., Ed.; ASM International: Materials Park, OH, 1989, p. 802.
2. Manzione, L. T. Plastic Packaging of Microelectronic Devices; Van Nostrand Reinhold: New York, 1990.

3. Baikerikar, K. K.; Scranton, A. B. Polymer, 2000, 42, 431.
4. Narayanan, V.; Scranton, A. B. Trends Polym Sci 1997, 5, 415.
5. Narayanan, V.; Baikerikar, K. K.; Scranton, A. B. RadTech '98 North America UV/EB Conference Proceedings, 1998, p. 31.
6. Baikerikar, K. K.; Scranton, A. B. Polym Compos 2000, 21, 297.
7. Parker, W. J.; Jenkins, R. J.; Butler, C. P., Abbott, G. L. J Appl Phys 1961, 32, 1679.
8. Kim, S. IEEE Trans CHMT 1991, 14, 809.
9. Schmidt, R. G.; Bell, J. P. Adv Polym Sci 1986, 75, 33.
10. Song, S. M.; Park, C. E.; Yun, H. K.; Oh, S. Y.; Park, J. M. J Adhesion Sci Technol 1997, 11, 797.
11. Goosey, M. T. Plastics for Electronics; Elsevier: New York, 1985.
12. Shin, D. K.; Lee, J. J. Adv Electron Pack (ASME) 1997, 1, 253.
13. Ho, T. H.; Wang, C. S. J Appl Polym Sci 1993, 50, 477.
14. Tummala, R. R.; Rymaszewski, E. J., Eds. Microelectronics Packaging Handbook; Van Nostrand Reinhold: New York, 1989.
15. Kinjo, N.; Ogata, M.; Nishi, K.; Kaneda, A. Adv Polym Sci 1989, 88, 5.
16. Michael, M.; Nguyen, L. Inter-Society Conf Thermal Phenom 1992, 246.
17. Agari, Y.; Uno, T. J Appl Polym Sci 1986, 32, 5705.
18. Hatta, H.; Taya, M. J Appl Phys 1985, 58, 7, 2478.
19. Hashin, Z.; Shtrikman, S. J Appl Phys 1962, 33, 1514.
20. Nielsen, L. E. Ind Eng Chem Fund 1974, 13, 17.
21. Bigg, D. M. Adv Polym Sci 1995, 119, 1.
22. Wong, C. P.; Bollampally, R. S. IEEE Trans Adv Pack 1999, 22, 1, 54.
23. Agari, Y.; Ueda, A.; Tanaka, M.; Nagai, S. J Appl Polym Sci 1990, 40, 929.
24. Schmidt, R. G.; Bell, J. P. Adv Polym Sci 1986, 75, 33.
25. Landrock, A. H. Adhesives Technology Handbook; Noyes Publications: Park Ridge, NJ, 1985.